This is a repository copy of *Grid-connected modular PV-Converter system with shuffled frog leaping algorithm based DMPPT controller*.

White Rose Research Online URL for this paper:
http://eprints.whiterose.ac.uk/123139/

Version: Accepted Version
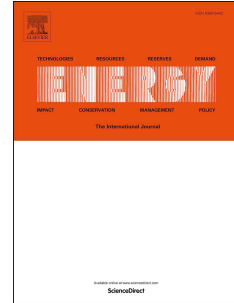
Accepted Manuscript

Grid-connected modular PV-Converter system with shuffled frog leaping algorithm based DMPPT controller

Mingxuan Mao, Li Zhang, Pan Duan, Qichang Duan, Ming Yang

Grid-Connected Modular PV-Converter System with Shuffled Frog Leaping Algorithm Based DMPPT Controller

Mingxuan Mao[1,2,*], Li Zhang[3], Pan Duan[4], Qichang Duan[1], Ming Yang[2]

[1]Automation College, Chongqing University, Chongqing 400044, China

[2]School of Electrical Engineering, Chongqing University, Chongqing 400044, China

[3]School of Electronic and Electrical Engineering, University of Leeds, Leeds LS2 9JT, United Kingdom

[4]State Grid Chongqing Electric Power Company Nan'an Power Supply Subsidiary Company,

Chongqing, China

Abstract: Maximum power extraction for PV systems with multiple panels under partial shading conditions (PSCs) relies on the configuration of the system and the optimal searching algorithms used. This paper described a PV system with multiple PV panels in series. Each panel has a dc-dc step-down converter, hence allowing independent control of load and source power ratio corresponding to the irradiation levels. An H-bridge terminal inverter is also used for grid connection. An advanced searching algorithm (TSPSOEM) is proposed in the paper for the distributed maximum power point tracking (DMPPT). This applies the basic particle swarm optimization (PSO) procedure but with an extended memory and incorporating the grouping concept from shuffled frog leaping algorithm (SFLA). The new algorithm is applied simultaneously to all PV-converter modules in the chain. The system can exploit the variable converter ratios and reduces the effect of differential shading, both between panels and across panels. The paper presents the system and the proposed new algorithm and demonstrating superior results obtained when compared with other conventional methods.

---

[*] Corresponding author, Tel.: +8615922927511, Fax:02365104819
Email address: mingxuan_mao@sina.com

Partial Shading Conditions (PSCs)

1 Introduction

Solar PV panels supply electricity to load nearby and utility grid [1]. All of these solar PV power generators are made by panels in serial and parallel strings to raise the voltage and current to the required standard levels and these panels are formed by having multiple chained PV cells. Series connected panels and cells are constrained to conduct the same string current which is set by the least efficient panel and cell, hence reducing the efficiency of the whole PV generator. Thus the PV panels and cells should, ideally, have the same rating and characteristics and operating under the same weather conditions. However, PV panels and cells in a string never operate exactly identical even if they are made from the same process, having the same size, and operating under the same orientation. The main issue is due to unequal lighting intensity across a PV panel [2]. If a subset of PV cells is shaded, the output characteristics of the PV source exhibits multiple local maximum power points (Local MPPs) as shown in Figure 1. The current through the panel must be limited to the maximum forward current in the shaded set to avoid driving any of these into a reverse voltage condition. This always absorbs power and can result in reverse breakdown and overheating. The use of by-pass diodes has eliminated this problem, but power potentially available from by-passed cells is lost.

To address this issue, attentions have been placed on two aspects: the connections and configurations of the PV system [3, 4] and the advanced MPPT techniques [5, 6]. The former uses different converter topologies combined with the PV panels which have been reported [4, 7-14]. This allows independent control of load and source power ratio corresponding to the irradiation levels and is particularly effective in addressing unequal shading between panels. The latter is useful to overcome the uneven shading across a single panel. Walker and Sernia in [4] have examined cascading multiple PV-converter units

using four types of dc-dc converters and their pros and cons. The work has shown that dc-dc step down converter is the most efficient. The system proposed by Abdalla et al. [10] uses step-down DC-DC converters for each PV panel to achieve independent control, but the MPPT used in this work is the conventional P&O method which cannot obtain the maximum power under PSCs of each PV string. The works in [7, 13-14] uses step-up (Boost) DC-DC converters for each PV module with independent MPPT control, but also applied conventional MPPT methods. The use of cascaded H-bridge has also been reported in [3, 7], this approach, though able to obtain independent control of PV panels, has the drawback of using many switches, hence making the control strategies complex and increasing power loss, cost.

The maximum power point tracking schemes are important in obtaining MPPT when a single PV panel being unevenly shaded, resulting in multiple peaks on the power-voltage characteristic curve. Conventional MPP searching algorithms [7, 15-21] may be trapped in a local maximum which indirectly introduce a power loss [22]. The work in developing the optimal searching methods and algorithms has been active, resulting in an avalanche of control and optimization strategies being reported in the literatures [22-34]. Among them, Particle Swarm Optimization (PSO) has been applied most frequently. This is due to that it can locate the MPPs compared with other methods such as Perturb & Observe (P&O), Incremental Conductance (IC), Hill Climbing (HC), Fuzzy Logic Controller (FLC), Neural Network (NN) etc., but PSO has problems in coping with fast variations of partial shading patterns. For this problem, different modifications have been made to the original PSO algorithm in order to improve its performance of tracking the global MPPT under PSCs. One approach used PSO to locate the nearest section where the global MPP may lie, and then used the conventional P&O or HC to find the exact point to reduce steady-state oscillation [14, 35]. The main defect of this approach lies in the determining the condition to switch over from PSO to P&O, unsuitable moment to switching over may incur inaccurate

results or increased computational cost. A hybrid PSO and Artificial Neural Network (PSO-ANN) algorithm was also proposed in [36] to detect the global peak power point in the presence of several local peaks. Although this method has advantage of relative high tracking accuracy, it is complex in developing NN hence more costly in sample training and computational time.

This paper presents a new grid-connected PV system which combines the chained PV-converter modules with an advanced MPPT algorithm. This combination enables the system to achieve MPPT for unequal shading between and across PV panels. In detail the system comprises a chain of integrated PV step-down dc-dc converter modules, hence generates multiple-levels of dc-voltage and may be converted to ac via a dc-ac converter. The control scheme is adopted from the proposed PSO algorithm with the grouping idea and extended memory factor and can search more accurately and effectively when multiple peaks occurs for a PV panel in the chain. Thus for n PV-converter modules there will be n MPPT searching schemes operating simultaneously. The predicted voltages are applied to control the corresponding dc-dc converters and dc-ac inverter simultaneously. Furthermore for the switch control of dc-dc converters of PV modules a permutation Pulse-Width Modulation (PWM) scheme is applied to allow switching sequence swapping for balanced switch utilisation. Finally, the output of the whole converter chain is connected to a dc-ac voltage source inverter, providing the ac output voltage synchronized with grid voltage.

The rest of the paper is organized as follows: In Section 2, configuration and model of the grid-connected cascaded PV-converter system are described. The system model and control is described in Section 3. In addition, the proposed maximum power point tracking scheme based on the TSPSOEM algorithm is presented in detail in Section 4. Section 5 presents and discusses the simulation results. Finally, we give the conclusion in Section 6.

2 Configuration of the Grid-connected Cascaded PV-Converter System

Figure 2 shows the configuration of a grid-connected PV system comprising three cascaded PV-step-down converter units. The proposed PV system is mainly made up of three PV panels, multilevel DC-link converters, one H-bridge inverter, a low-pass R-L filter, grid and a control unit. Specifically, each of PV panels can be made up of n chained PV modules, though in this work three PV modules (Module$_1$, Module$_2$ and Module$_3$) are used. Furthermore, three converter switches (SWn, n=1, 2, 3) are controlled by the direct PWM method to form a three-level positive DC voltage, which is converted to alternating voltage at the required grid frequency of 50 Hz by the H-bridge inverter [10]. Connection to the grid is through a low-pass R-L filter for eliminating high order harmonics due to switching.

3 System Model and Control

3.1 State-Space Average (SSA) Model

The state-space average (SSA) model expressing the dynamic variation of the above system can be derived as follows. The voltages across each of the dc-dc converter terminals, v_{D1}, v_{D2}, …v_{Dn}, can be expressed as functions of their respective PV source voltages, v_{pv1}, v_{pv2}, …v_{pvn} and the corresponding switching duty ratios D_1, D_2, …D_n, thus we have

$$v_{Dn} = D_n \cdot v_{PVn} \tag{1}$$

The currents through capacitors across each PV sources C_{pv1}, C_{pv2}, $\cdots C_{pvn}$ are determined by their respective PV source currents (i_{pv1}, i_{pv2}, $\cdots i_{pvn}$) and that flowing to the DC-link (i_{link}) and converter duty ratios.

$$i_{c_{PVn}} = C_{PVn} \frac{dv_{PVn}}{dt} = i_{PVn} - i_{link} \cdot D_n \tag{2}$$

Assuming a resistive load is supplied, the current to the DC-link, is given as

$$i_{link} = \frac{v_{D1} + v_{D2} + v_{D3} + \cdots v_{Dn}}{R} \tag{3}$$

Substituting i_{link} in eqs. (2) by (3), we have

$$\frac{dv_{PVn}}{dt} = \frac{1}{C_{PVn}}\left(i_{PVn} - \frac{v_{D1} + v_{D2} + \cdots v_{Dn}}{R}D_n\right) \tag{4}$$

The output voltage is determined by the DC-link voltage and switching state of the output H-bridge as

$$v_{out} = (v_{D1} + v_{D2} + v_{D3} + \cdots v_{Dn})|\sin(\omega t \pm \delta)| \cdot (2S - 1) \tag{5}$$

where S is the switch state ('0' for off state and '1' for on state) of the H-bridge, δ represents the sinusoidal signal phase shift angle between the current from the PV system and grid voltage.

Hence the general form of the SSA model for this system with n cascaded PV-converter modules is given as

$$\begin{bmatrix} \dfrac{dv_{pv1}}{dt} \\ \dfrac{dv_{pv2}}{dt} \\ \cdot \\ \cdot \\ \cdot \\ \dfrac{dv_{pv(n)}}{dt} \end{bmatrix} = \frac{1}{R}\begin{bmatrix} \dfrac{-D_1^2}{C_{pv1}} & \dfrac{-D_1 D_2}{C_{pv1}} & \cdot & \cdot & \cdot & \dfrac{-D_1 D_n}{C_{pv1}} \\ \dfrac{-D_2 D_1}{C_{pv2}} & \dfrac{-D_2^2}{C_{pv2}} & \cdot & \cdot & \cdot & \dfrac{-D_2 D_n}{C_{pv2}} \\ \cdot & \cdot & \cdot & \cdot & \cdot & \cdot \\ \cdot & \cdot & \cdot & \cdot & \cdot & \cdot \\ \cdot & \cdot & \cdot & \cdot & \cdot & \cdot \\ \dfrac{-D_n D_1}{C_{pv(n)}} & \dfrac{-D_n D_2}{C_{pv(n)}} & \cdot & \cdot & \cdot & \dfrac{-D_n^2}{C_{pv(n)}} \end{bmatrix}\begin{bmatrix} v_{pv1} \\ v_{pv2} \\ \cdot \\ \cdot \\ \cdot \\ v_{pv(n)} \end{bmatrix} + \begin{bmatrix} \dfrac{1}{C_{pv1}} & 0 & \cdot & \cdot & \cdot & 0 \\ 0 & \dfrac{1}{C_{pv2}} & 0 & \cdot & \cdot & 0 \\ 0 & 0 & \cdot & 0 & \cdot & \cdot \\ 0 & 0 & 0 & \cdot & 0 & \cdot \\ 0 & 0 & 0 & 0 & \cdot & 0 \\ 0 & 0 & 0 & 0 & 0 & \dfrac{1}{C_{pv(n)}} \end{bmatrix}\begin{bmatrix} i_{pv1} \\ i_{pv2} \\ \cdot \\ \cdot \\ \cdot \\ i_{pv(n)} \end{bmatrix} \tag{6}$$

$$\begin{bmatrix} v_{out} \end{bmatrix} = (2S - 1)\begin{bmatrix} D_1 & D_2 & \cdots & D_n \end{bmatrix}\begin{bmatrix} v_{pv1} \\ v_{pv2} \\ \vdots \\ v_{pv(n)} \end{bmatrix}|\sin(\omega t \pm \delta)| \tag{7}$$

For ac part the output current flow can be expressed as

$$L\frac{d\vec{i_G}}{dt} = \vec{v}_{out} - \vec{v}_G - R_f\vec{i_G} \tag{8}$$

where i_G and v_G represent the grid current and voltage respectively, R_f and L are the filter resistance and inductor.

3.2 PWM Control Scheme

As shown in Figure 2, the control unit of the grid-connected PV system includes an MPPT block for each PV-converter unit. The output signals of these blocks are multiplied by a unity sinusoidal signal to form AC reference signals $v_{ref(j)}$, j=1,2,3…n. These reference signals are used to control the inverter switches by applying the direct PWM (the first stage in the algorithm) and the output generation. The direct PWM normalized reference voltage is given as

$$\bar{v}_{ref(j)} = \frac{|v_{ref(j)}|}{V_{mpp}/n} \tag{9}$$

where V_{mpp} is the MPP voltage of a PV source at irradiance of 1000 W/m^2, and n denotes the total number of PV sources.

The integer part of the normalized reference voltage is defined as the normalized offset voltage and it is given as

$$v_{offset(j)} = int[\bar{v}_{ref(j)}] \tag{10}$$

The t_{on} interval of the PV source, which is being controlled at a particular switching period, is given as

$$t_{on(j)} = T_c \cdot (\bar{v}_{ref(j)} - v_{offset(j)}) \tag{11}$$

Equation (11) can be derived by equating the approximated volt-time area of the graph '$v_{ref(j)}$ vs. time' with the corresponding area under the generated pulse within a cycle T_c [37].

Figure3 shows the flowchart of the PV permutation algorithm [10] which is applied to the three PV sources.

3.3 Power Flow Control

The current flow to the grid should ideally be maintained to be in phase with the grid voltage. This is achieved by using a simple quarter cycle delay phase locking loop [38] to track the grid voltage phase angle, and adjust the sinusoidal signal phase shift angle δ in eq. (5). Taking grid voltage as reference, the real power flow to the grid is

$$P = i_G v_G \tag{12}$$

When the system ac output voltage leads the grid voltage with phase angle evaluated as

$$\delta = tan^{-1} \frac{i_G \omega L}{|v_G| + R_f i_G} \tag{13}$$

where $|v_G|$ represents RMS of the grid voltage. Note δ angle changes with the output current and is calculated at every sample instant according to the estimated maximum power.

4 Maximum Power Point Tracking Scheme

The proposed PSO-based MPPT algorithm (TSPSOEM) offers the feature of extended memory searching capabilities and incorporates the grouping idea of shuffled frog leaping algorithm (SFLA) [39]. It reduces voltage ripple and increases the power output under PSCs. With the PV system of multiple chained PV-converter modules shown in Figure 2, the algorithm is applied to each of the n modules simultaneously to track their respective MPPs. The procedure and equations of this algorithm are detailed below.

4.1 Principles of the basic PSO Algorithm

PSO [40] is an evolutionary computation technique proposed by Kennedy and Eberhart in 1995. In PSO, A set of randomly placed particles is initialized; each particle represents a potential solution and has a corresponding fitness value derived from a fitness function. The objective is to find the optima by updating generations of particles. Assuming a space containing S particles, the updating velocities and positions of the particles at the tth iteration are respectively denoted as v^t and x^t. In the iterative process, the updated position of this particle at the $(t+1)^{th}$ time step is influenced by the information of its own best position p_l^t and the global best p_l^g at the tth step. The velocity and particle position update formulas are written as follows:

$$v^{t+1} = \omega v^t + c_1 r_1 \left(p_l^t - x^t \right) + c_2 r_2 \left(p_g^t - x^t \right) \tag{14}$$

$$x^{t+1} = x^t + v^{t+1}$$

(15)

where ω is the inertia weight factor, its variation range is chosen by the users. t is the iteration order, c_1 and c_2 are the acceleration factors, r_1, r_2 are random values $\in (0, 1)$. To prevent the resultant particles moving out of range, their velocities and positions are limited to the ranges defined respectively by $[v_{min}, v_{max}]$ and $[x_{min}, x_{max}]$.

Applying the PSO algorithm to search the MPPs of a PV array the particles are the PV terminal voltages. The fitness value for each particle (voltage) is the output power of the PV array which is evaluated using a simplified form of original Bishop model [41] defined as

$$I_{out} = I_{sc} - I_o \left[\exp\left(\frac{qV_j}{AKT_c} \right) - 1 \right] - I_{shunt}$$

(16)

$$FitnessFunction = Power(G, T, I_{out}) = I_{out} \times V_{out}$$

(17)

where I_{sc} is the photo current, the second current on the RHS formula is due to P-N junction leakage, V_j is the P-N junction voltage and I_{shunt} represents the PV panel ohmic leakage current. Definitions of other parameters in eq. (16) are given in the Appendix.

The shortcoming of the basic PSO algorithm is that it cannot cope well for the maximum power point searching of a PV system under unequal and changing illumination conditions. With multiple optimal points, for fast and accurate searching for maxima, the algorithm needs a large population size to cover a wide area which is certain to contain all the optima. In addition the searching velocity cannot be too high in case it misses the optimal particle. Hence the algorithm is slow to converge. On the other hand a larger searching velocity may result in low precision and a relapse into local optimization.

4.2 Improved PSO Algorithm

An extended memory factor is introduced into the basic PSO algorithm [42] to increase the accuracy of maximum power point tracking. This is realized by combining the local and global maxima obtained from

the last iteration with those of the current process, so that the influence of previous result can be maintained, i.e. the search process has an extended memory. The equation for the new searching speed is expressed as

$$v^{t+1} = \omega v^t + c_1 r_1 \left[\xi^t \left(p_l^t - x^t \right) + \xi^{t-1} \left(p_l^{t-1} - x^{t-1} \right) \right] + c_2 r_2 \left[\xi^t \left(p_g^t - x^t \right) + \xi^{t-1} \left(p_g^{t-1} - x^{t-1} \right) \right] \qquad (18)$$

where p_l^{t-1} represents current local extreme position of the particle in the $(t-1)^{th}$ iterative process; p_g^{t-1} is the current global extreme position of the population in the $(t-1)^{th}$ iterative process; ξ^t is called current effective factor; ξ^{t-1} the effective factor of the extended memory, and $x_{t+1}=x_t+v_{t+1}, \xi, \xi^{-1} \in R^+, \xi + \xi^{-1}=1$. In the special case when $\xi^{-1}=0$, that is, $\xi=1$, eq. (18) is equal to eq. (14), hence resulting no extended memory.

4.3 Proposed PSO Algorithm with SFLA (TSPSOEM)

This takes into account the specific feature of a PV generation system operating under PSCs, namely that the P-V characteristic exhibits multiple peaks as shown in Figure 1. The number of these peaks depends on the number of chained modules and their respective illumination levels, and only one of them corresponds to the global MPP. SFLA is a meta-heuristic algorithm, which has been considered ideal for tracking maximum power point in PV system during partially shaded conditions due to its special features in [30]. Therefore, to further address the issue under PSCs, the grouping idea of SFLA and extended memory factor are merged into the basic PSO algorithm to track the global MPP for partially shading PV panel. The procedure and the equations used are detailed as follow.

Stage (1): All particles are divided into several groups according to the grouping idea of the SFLA. Within each group the extended memory factor is applied for speed evaluation for each particle. Thus with the local best already obtained, the speed and position of each particle of the nth particle in the mth group are updated using the equations:

$$v_{mn}^{t+1} = \omega v_{mn}^t + c_1 r_1 \left[\xi^t \left(P_m^t - x_{mn}^t \right) + \xi^{t-1} \left(P_m^{t-1} - x_{mn}^{t-1} \right) \right] \qquad (19)$$

$$x_{mn}^{t+1} = x_{mn}^t + v_{mn}^{t+1} \qquad (20)$$

$$\omega = \omega_{\max} - \left(\omega_{\max} - \omega_{\min}\right)\frac{K}{J} \tag{21}$$

where $m = 1, 2, \ldots, M$ being the number of groups, *and* $n = 1, 2, \ldots, N$, where N is the number of particles within a group. P^t_m and P^{t-1}_m are, respectively the best particle positions in the mth group at the tth, and the $(t\text{-}1)^{th}$ iterations. Having obtained n particle positions at the $(t+1)^{th}$ step, we evaluate their fitness values using eqs. (16) and (17) and then acquire the best particle. Subsequently, a new local best position for the mth group, P_m, is derived. For eq. (21), K is the generation index representing the current number of evolutionary generations, and J is a predefined maximum number of generations. The maximal and minimal weights ω_{max} and ω_{min} have been set to 0.9 and 0.4.

Stage (2): Using m local best particles to find the one giving the maximum power amongst them, this is chosen as the optimal for the entire population at the kth iteration step, i.e the global best. Furthermore the global best position in the last iteration is added. The speed and position of the current best particles are updated by the formulas:

$$v^{t+1}_m = c_2 r_2 \left[\left(P^t_g - P^t_m\right) + \left(P^{t-1}_g - P^{t-1}_m\right)\right] \tag{22}$$

$$P^{t+1}_m = P^t_m + v^{t+1}_m \tag{23}$$

where P^t_g is the best position of particles in the entire swarm at the kth iteration, P^{t-1}_g is the best position of particles in the entire swarm at the kth iteration.

In the iterative procedure, when the best value within a group is equal to the global best value, the $(P_g\text{-}P_m)$ in eq. (22) is zero. The iterative process converges. The algorithm also stops when a fixed iteration count J is reached.

4.4 Implementation Procedure

The flowchart for implementing the proposed algorithm is shown in Figure 4. This MPPT method is applied in sequence to each PV unit at each sampling instant, to track their respective reference voltages.

This may lead to different voltage values depending on the weather conditions for each PV panel.

The specific process of the proposed MPPT method is shown as follows:

i) Input the current temperature (T) and light intensity (G) and initialize the positions and speeds of all particles;

ii) Calculate the fitness values using eqs. (16) and (17) for each particle;

iii) Apply the SFLA concept to partition the particles into several groups according fitness values;

iv) Search for the peak power point in each group by using eqs. (19)-(21);

v) Shuffle all the local best particles in the groups with each other, and find the one giving the maximum power amongst them, i.e. the global best, using eqs. (22) and (23);

vi) Check the (P_g-P_m) in eq. (22), if it is zero, the process converges and program ends,

vii) Check the specified number of iterations to exit the program and output the optimal position (V_{ref}), otherwise return to step ii).

5 Simulation Results and Discussion

5.1 Output power control under static shading conditions

Simulations were performed of a system having three serially connected identical PV-converter units and a dc-ac inverter at the output as shown in Figure 2. The parameters of the system components are listed in Table 1. The measured P-V characteristic curves of the PV panels (sources) are shown in Figure5 under different irradiance levels at a surface temperature of 20°C, and show single or multiple peaks corresponding to different shading patterns.

To evaluate the performance of the proposed MPPT control method, the resulting output current, voltage and power are compared with those from the basic P&O method and the traditional PSO method under two shading patterns. The P&O method is set at a fixed step size (e_v =0.1V), and the main

parameters used in the traditional PSO method and the proposed TSPSOEM method are listed in Table 2. In addition, the Fast Fourier Transform (FFT) is used to analyze the harmonic components present in the output waveform and the total harmonic distortion (THD) factors for all cases are evaluated.

Two test cases are considered as shown in Table 3. Case 1: Irradiance levels are only different between the PV panels, but are constant across each panel, i.e. the uniform shading case. Case 2: Light levels vary across each of the three panels, so it is non-uniform shading. As can be seen in Table 3, in Case 1, G_1, G_2 and G_3 represent the irradiance levels on panels PV_1 PV_2 and PV_3, while, in Case 2, G_{1x}, G_{2x} and G_{3x} are the irradiance levels of the three chained PV modules within each PV panel.

Figure 6 shows the output I/V waveforms and the total average power delivered to the grid corresponding to each method for the two cases: (a) shows the results for Case 1 and (b) for Case 2. The powers extracted from the sources by each of the three methods are shown by line graphs on the right-hand side (column 4), and compared to the theoretical maximum power extractable when the three modules operate independently under the same shading conditions. Clearly the proposed new method generates more power than the other two, since its power curves in both cases are the closest to the maximum power achievable given by P_{PV}. Figure 7 shows the grid-side sinusoidal current and voltage obtained by using the proposed TSPSOEM method under the illumination condition defined in Case 2. They are in phase as desired.

Table 4 lists the results from each method in terms of generated power and THD. It can be seen from the figures and Table 4 that the proposed method generates consistently higher power than the other two methods. Compared to the maximum power achievable under the same weather conditions, the power extraction percentage for the new method can be as high as 98%. In addition, when three methods run 10 times independently under the same conditions, the proposed method not only always shows the highest success rate (SR) of tracking the maximum power point, but also shows the lowest THD according to the

measured current, indicating the best waveform performance.

5. 2 Output power control under variable shading conditions

This is to evaluate the performance of the proposed method under fast changing weather conditions. Starting with illumination levels set uniformly at 1000W/m^2 for all three panels, three different illumination patterns as listed in Table 5 are applied. The parameters of this system and the MPPT methods applied are the same as those listed in Tables 1-2. Figures 8 shows the power delivered to the grid using these two methods under Cases 2, 3, 4. The total generated power P_{PV} for the case when the three PV-converter units operate separately is again used for comparison. As can be seen, at t = 0.5 sec. the illumination pattern changes from the initial setting to that of Case 2, the three power values respond promptly and uniformly to this change, but the power level due to the proposed method is higher than for the PSO though it is lower than P_{PV}. Similarly when the illumination pattern changes to that specified in Case 3 at t = 1sec and Case 4 at t = 1.5 sec, the performances of the power responses for all methods are similar except that the new method always gives higher values than the PSO method.

The quantitative comparison between the two methods, including generated power, power extraction percentage (Rate) and THD of the current and voltage is summarized in Table 6. It can be seen that the proposed method generates consistently higher power than the PSO method, and the power extraction rate is also higher, notably 95.7% under the most serious shading pattern of Case 4. The method also shows lower THD according to the measured current, indicating the best waveform performance. From Figure 8 and Table 6 it is obvious that the proposed algorithm is superior in convergence accuracy under different partial shading patterns. The method can reduce the energy loss and significantly increase the output power.

6 Conclusions

This paper described a PV system with multiple chained PV-converter modules, and an H-bridge terminal inverter for grid connection. The example presented gives seven-level AC output. This structure

allows independent control of panels according to their light conditions. A new maximum power point search algorithm, named TSPSOEM, has been proposed. Applying this to the chained PV-converter configuration and combining with a permutation PWM algorithm, the system exploits the variable converter ratios and reduces the effect of differential shading, both between panels and across panels. The new MPPT algorithm is an improved PSO algorithm. Its two main features are: i) having an extended memory for optimal power searching, i.e. the search result from last iteration is used to adjust the current result, hence improving the search stability and increasing accuracy; ii) Applying the grouping idea of SFLA, hence speed up the convergence rate. TSPSOEM has been shown to search for the MPPs quickly and accurately and can reduce the voltage and current harmonics. The performance of the proposed algorithm has been compared to that of the conventional P&O and PSO schemes when controlling the chained PV-converter system under the same shading conditions. The new algorithm has shown extracting persistently higher power from the PV panels than its two counterparts in both static and variable shading condition. The maximum power extraction rate can reach a high 95.7%.

Acknowledgements

Appendix

Parameters of the Fitness Function used in the proposed MPPT method:

I_{sc}, I_{shunt}, and V_{out} are expressed in eqs. (24-26) as follow:

$$I_{sc} = \left\{ I_{scr} + k_i (\mathrm{T_c} - \mathrm{T_r}) \right\} * G \tag{24}$$

$$I_{shunt} = \frac{V_j}{R_p}\left\{1 + a\left(1 - \frac{V_j}{V_{br}}\right)^{-m}\right\} \tag{25}$$

$$V_{out} = V_j + R_s I_c \tag{26}$$

Diode ideality factor (A): 1.72;

Electron charge (q): 1.609×10^{-19}C;

Cell absolute temperature (T_c): $T_c = T + 273 + 0.2*G$;

Fixed cell series resistance (R_s): 5e-5Ω;

Fixed cell parallel resistance (R_p): 5e5Ω;

Temperature coefficient of the short-circuit current (k_i): 1.380658e-23A;

Reference temperature (T_r): 301.18 K°;

Short-circuit current (I_{scr}): 3.3A;

Reverse saturation current (I_o): 19.9693e-6A;

Junction breakdown voltage (V_{br}): -4.0V;

Fraction of ohmic current (a): 0.1;

Avalanche breakdown exponent (m): 3.7.

References

[1] Kannan N, Vakeesan D. Solar energy for future world: a review. Renew Sustain Energy Rev 2016;62:1092-105.

[2] Chin VJ, Salam Z, Ishaque K. Cell modelling and model parameters estimation techniques for photovoltaic simulator application: a review. Appl Energy 2015;154:500-19.

[3] Hasan R, Mekhilef S, Seyedmahmoudian M, et al. Grid-connected isolated PV microinverters: A review. Renew Sustain Energy Rev 2017;67:1065-1080.

[4] Walker GR, Sernia PC. Cascaded DC-DC converter connection of photovoltaic modules. IEEE Trans

Power Electron 2004;19:1130-1139.

[5] Liu L, Meng X, Liu C. A review of maximum power point tracking methods of PV power system at uniform and partial shading. Renew Sustain Energy Rev 2016;53:1500-7.

[6] Mellit A, Kalogirou S A. MPPT-based artificial intelligence techniques for photovoltaic systems and its implementation into field programmable gate array chips: Review of current status and future perspectives. Energy 2014;70:1-21.

[7] Prabaharan N, Palanisamy K. Analysis and integration of multilevel inverter configuration with boost converters in a photovoltaic system. Renew Sustain Energy Rev 2016;128:327-342.

[8] Saranrom W, Polmai S. The efficiency improvement of series connected PV panels operating under partial shading condition by using per-panel DC/DC converter. In: 2011 IEEE Conference on Electrical Engineering/Electronics, Computer, Telecommunications and Information Technology, ECTICON. p. 760-763.

[9] Bratcu AI, Munteanu I, Bacha S, et al. Power optimization strategy for cascaded dc-dc converter architectures of photovoltaic modules. In: 2009 IEEE Conference on Industrial Technology, ICIT. p. 1-8.

[10] Abdalla I, Corda J, Zhang L. Optimal control of a multilevel DC-link converter photovoltaic system for maximum power generation. Renew Energy 2016;92:1-11.

[11] Abolhasani MA, Rezaii R, Beiranvand R, et al. A comparison between buck and boost topologies as module integrated converters to mitigate partial shading effects on PV arrays. In: 2016 IEEE Conference on Power Electronics and Drive Systems Technologies, PEDSTC. p. 367-372.

[12] Khan O, Xiao W. An efficient modeling technique to simulate and control submodule-integrated PV system for single-phase grid connection. IEEE Trans Sustain Energy, 2016;7: 96-107.

[13] Bratcu AI, Munteanu I, Bacha S, et al. Cascaded dc–dc converter photovoltaic systems: Power optimization issues. IEEE Trans Ind Electron 2011;58:403-411.

[14] Poshtkouhi S, Biswas A, Trescases O. DC-DC converter for high granularity, sub-string MPPT in photovoltaic applications using a virtual-parallel connection. In: 2012 IEEE Conference on Applied Power Electronics Conference and Exposition, APEC. p. 86-92.

[15] Mozaffari Niapour SAKH, Danyali S, Sharifian MBB, Feyzi MR. Brushless DC motor drives

supplied by PV power system based on Z-source inverter and FLIC MPPT controller. Energy Convers Manage 2011;52:3043-59.

[16] Boukenoui R, Ghanes M, Barbot JP, et al. Experimental assessment of maximum power point tracking methods for photovoltaic systems. Energy 2017; 132: 324-340.

[17] Hong CM, Ou TC, Lu KH. Development of intelligent MPPT (maximum power point tracking) control for a grid-connected hybrid power generation system. Energy 2013; 50(50):270-279.

[18] Messai A, Mellit A, Massi Pavan A, Guessoum A, Mekki H. FPGA-based implementation of a fuzzy controller (MPPT) for photovoltaic module. Energy Convers Manage 2011;52:2695-704.

[19] Tsang KM, Chan WL. Three-level grid-connected photovoltaic inverter with maximum power point tracking. Energy Convers Manage 2013;65:221-7.

[20] Guenounou O, Dahhou B, Chabour F. Adaptive fuzzy controller based MPPT for photovoltaic systems. Energy Convers Manage 2014;78:843-850.

[21] Ahmed J, Salam Z. An improved perturb and observe (P&O) maximum power point tracking (MPPT) algorithm for higher efficiency. Appl Energy 2015;150:97-108.

[22] Ram JP, Rajasekar N. A new global maximum power point tracking technique for solar photovoltaic (PV) system under partial shading conditions (PSC). Energy 2017;118:512-525.

[23] Punitha K, Devaraj D, Sakthivel S. Artificial neural network based modified incremental conductance algorithm for maximum power point tracking in photovoltaic system under partial shading conditions. Energy 2013; 62(6):330-340.

[24] Rajesh R, Mabel MC. Design and real time implementation of a novel rule compressed fuzzy logic method for the determination operating point in a photo voltaic system. Energy 2016; 116:140-153.

[25] Letha SS, Thakur T, Kumar J, et al. Harmonic elimination of a photo-voltaic based cascaded H-bridge multilevel inverter using PSO (particle swarm optimization) for induction motor drive. Energy 2016; 107:335-346.

[26] Fathabadi H. Novel fast dynamic MPPT (maximum power point tracking) technique with the capability of very high accurate power tracking. Energy 2016; 94:466-475.

[27] Stefan D, Dorin P, Cristina M. A novel MPPT (maximum power point tracking) algorithm based on a modified genetic algorithm specialized on tracking the global maximum power point in photovoltaic

systems affected by partial shading. Energy 2014; 74(5):374-388.

[28] Fathabadi H. Novel highly accurate universal maximum power point tracker for maximum power extraction from hybrid fuel cell/photovoltaic/wind power generation systems. Energy 2016; 116:402-416.

[29] Manickam, C, Raman, GR, Raman, GP, Ganesan, SI, Nagamani, C. A Hybrid Algorithm for Tracking of GMPP Based on P&O and PSO With Reduced Power Oscillation in String Inverters. IEEE Trans Ind Electron 2016;63:6097-6106.

[30] Sridhar R, Jeevananthan S, Dash SS, et al. A new maximum power tracking in PV system during partially shaded conditions based on shuffled frog leap algorithm. J Exp Theor Artif In 2017;29:481-493.

[31] Sawant PT, Lbhattar PC, Bhattar CL. Enhancement of PV system based on artificial bee colony algorithm under dynamic conditions. In: 2016 IEEE Conference on Recent Trends in Electronics, Information & Communication Technology, RTEICT. p. 1251-1255.

[32] Seyedmahmoudian, M, Rahmani, R, Mekhilef, S, Oo, AMT., Stojcevski, A, Soon, TK, Ghandhari, AS. Simulation and hardware implementation of new maximum power point tracking technique for partially shaded PV system using hybrid DEPSO method. IEEE Trans Sustain Energy 2015;6:850-862.

[33] Mohammed S S, Devaraj D, Ahamed T P I. A novel hybrid Maximum Power Point Tracking Technique using Perturb & Observe algorithm and Learning Automata for solar PV system. Energy 2016;112:1096-1106.

[34] Bizon N. Searching of the extreme points on photovoltaic patterns using a new Asymptotic Perturbed Extremum Seeking Control scheme. Energy Convers Manage 2017;144:286-302.

[35] Ishaque, K, Salam, Z, Amjad, M, Mekhilef, S. An improved particle swarm optimization (PSO)–based MPPT for PV with reduced steady-state oscillation. IEEE Trans Power Electron 2012;27:3627-3638.

[36] Ngan, MS, & Tan, CW. Photovoltaic Multiple Peaks Power Tracking Using Particle Swarm Optimization with Artificial Neural Network Algorithm. In: Advances in Solar Photovoltaic Power Plants, 2016. p. 107-138.

[37] Dai NY, Wong MC, Chen YH, et al. A 3-D generalized direct PWM algorithm for multilevel

converters. IEEE Power Electron Lett 2005;3:85-88.

[38] Zhong QC, Hornik T. Control of power inverters in renewable energy and smart grid integration. John Wiley & Sons, 2012.

[39] Eusuff, MM, and Lansey, KE. Optimization of water distribution network design using the shuffled frog leaping algorithm. J Water Res Plan Man 2003;129:210-225.

[40] Eberhart, R, and Kennedy, J. A new optimizer using particle swarm theory. In: 1995 Proceedings of the Sixth International Symposium on Micro Machine and Human Science, p. 39-43.

[41] Bishop, JW. Computer Simulation of the Effects of Electrical Mismatches in Photovoltaic Cell Interconnection Circuits. Sol Cells 1998;25:73-89.

[42] Duan, QC, Huang, DW, Lei, L and Duan, P. Simulation analysis of particle swarm optimization algorithm with extended memory. Contr Dec 2011;26:1087-1100.

Tables:

Table 1PV system parameters used in simulations

Symbol	Parameter	Value
P_{mpp}	Maximum power of one PV module	15W
C_{pv}	PV source terminal capacitor	2200μF
V_{oc}	Open circuit voltage	6.6V
I_{sc}	Short circuit current	3.28A
L_1, L_2	inductance	1mH
R_1, R_2	resistance	0.1Ω
e_v	P&O tracking step size	0.1 V
M_f	Frequency modulation index	150
f	AC output frequency	50Hz

Table 2Parameter setting of the PSO and proposed methods

Method	c_1	c_2	ω	Gene.	S	M	ξ_{t-1}	ξ_t
PSO	0.6	0.8	0.9	3	12	--	--	--
TSPSOEM	0.6	0.8	self-adaption ($\omega_{max}=0.9, \omega_{min}=0.4$)	3	12	3	0.5	0.5

Table 3 Different Irradiance level in two cases

Case	T=20□								
	G_1 (W/m^2)			G_2 (W/m^2)			G_3 (W/m^2)		
1	1000			700			400		
	G_{11}	G_{12}	G_{13}	G_{21}	G_{22}	G_{23}	G_{31}	G_{32}	G_{33}
2	1000	800	400	1000	700	1000	1000	1000	200

Table 4 Summary of simulated results under different partial shading conditions

Case	P_{pv}(W)	P&O algorithm				PSO algorithm				Proposed algorithm			
		Power (W)	Rate* (%)	THD (%)	SR# (%)	Power (W)	Rate (%)	THD (%)	SR (%)	Power (W)	Rate (%)	THD (%)	SR (%)
1	64.4	60.3	93.6	39.16	80	60.6	94.1	41.56	90	63.1	98.0	32.37	100
2	64.8	60.4	93.2	45.33	40	62.0	95.7	32.44	70	63.9	98.6	32.58	100

*Rate = actual power as percentage of theoretical maximum P_{PV}.

#SR = success rate of tracking the maximum power point (P_{max}).

Table 5 Variation value of each case of irradiance and phase angle

Case	T=20℃								
	G_1 (W/m^2)			G_2 (W/m^2)			G_3 (W/m^2)		
1	1000			1000			1000		
	G_{11}	G_{12}	G_{13}	G_{21}	G_{22}	G_{23}	G_{31}	G_{32}	G_{33}
	(W/m^2)			(W/m^2)			(W/m^2)		
2	900	400	700	1000	500	800	1000	1000	1000
3	1000	1000	1000	1000	500	1000	1000	1000	700
4	900	700	500	1000	700	400	1000	500	1000

Table 6 Summary of output results with two methods under fast variations of shading patterns

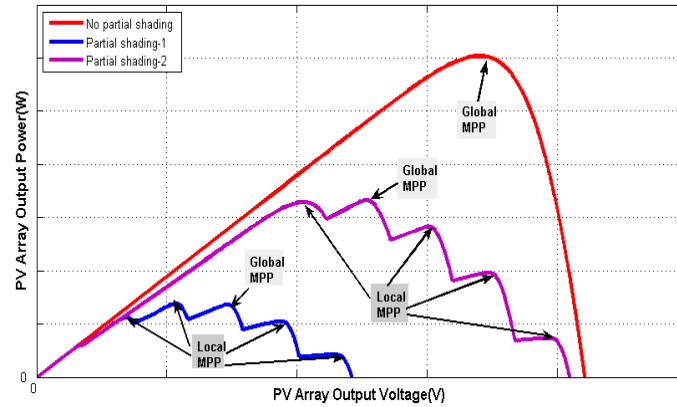| Case	P_{pv} (W)	PSO method				TSPSOEM method			
		Power(W)	Rate(%)	THD$_{(V)}$ (%)	THD$_{(I)}$ (%)	Power(W)	Rate(%)	THD$_{(V)}$ (%)	THD$_{(I)}$ (%)
1	120.50	104.21	86.5	25.86	8.24	104.21	86.5	25.86	8.24
2	67.53	60.95	90.3	30.25	8.31	62.24	92.2	29.23	8.26
3	88.06	78.10	88.7	27.89	8.61	81.05	92.0	27.83	7.44
4	58.57	53.92	92.1	27.42	7.57	56.04	95.7	26.78	8.04

Figures:

Figure 1 Examples of the P-V characteristics curves of a PV array composed of series-connects PV modules for the different irradiations.
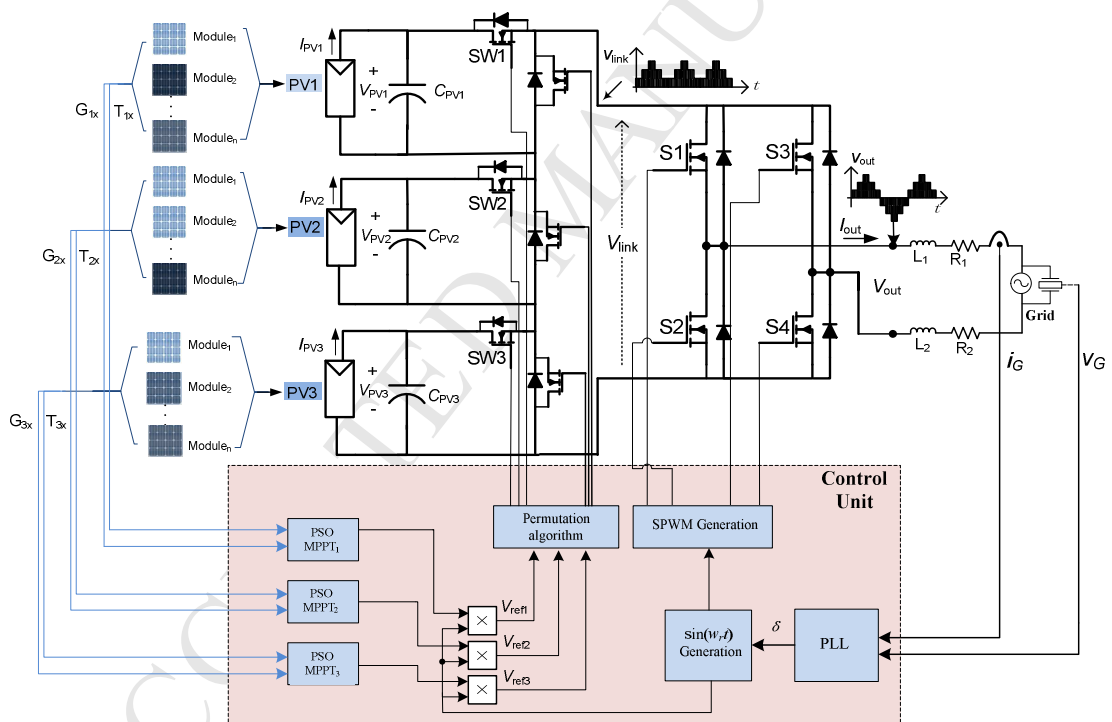

Figure 2 Structure of the grid-connected PV system with seven-level DC-link converter and the proposed MPPT method
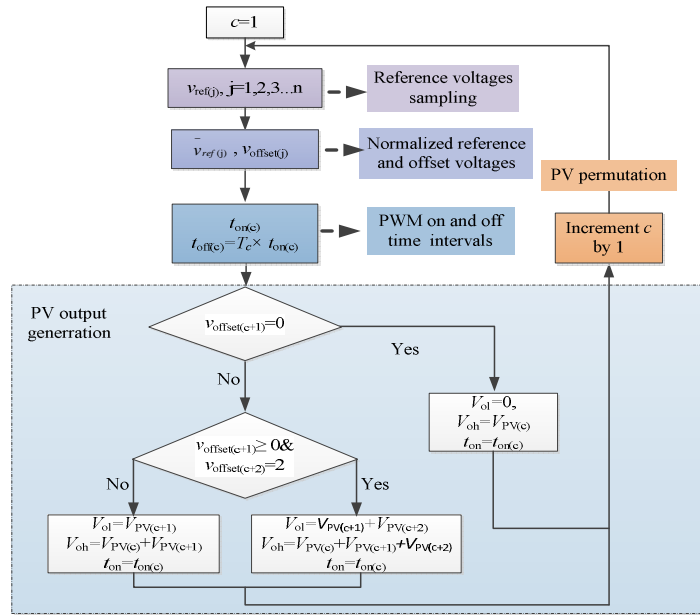
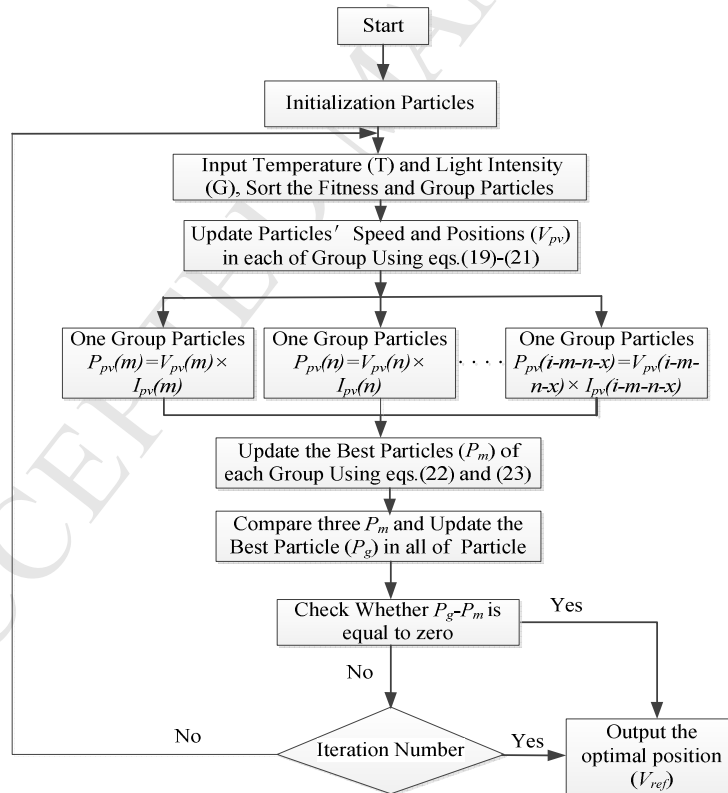Figure 3 Flowchart of the PV permutation algorithm for seven-level inverter

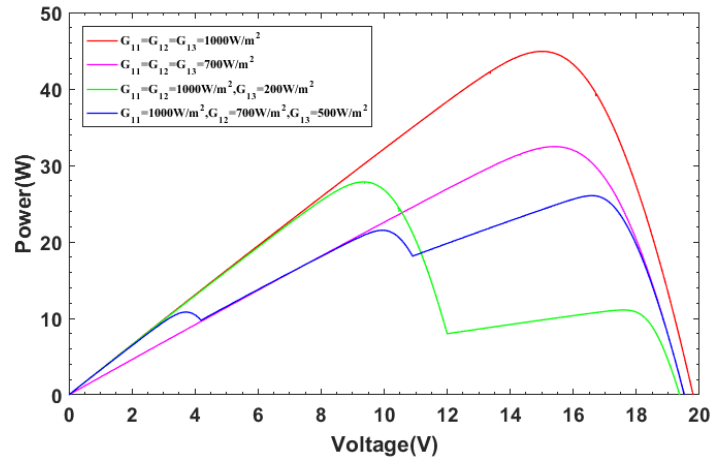Figure 4 Flowchart of the proposed MPPT method

Figure 5 Measured P-V curves of one PV panel (source) under different partial shading patterns
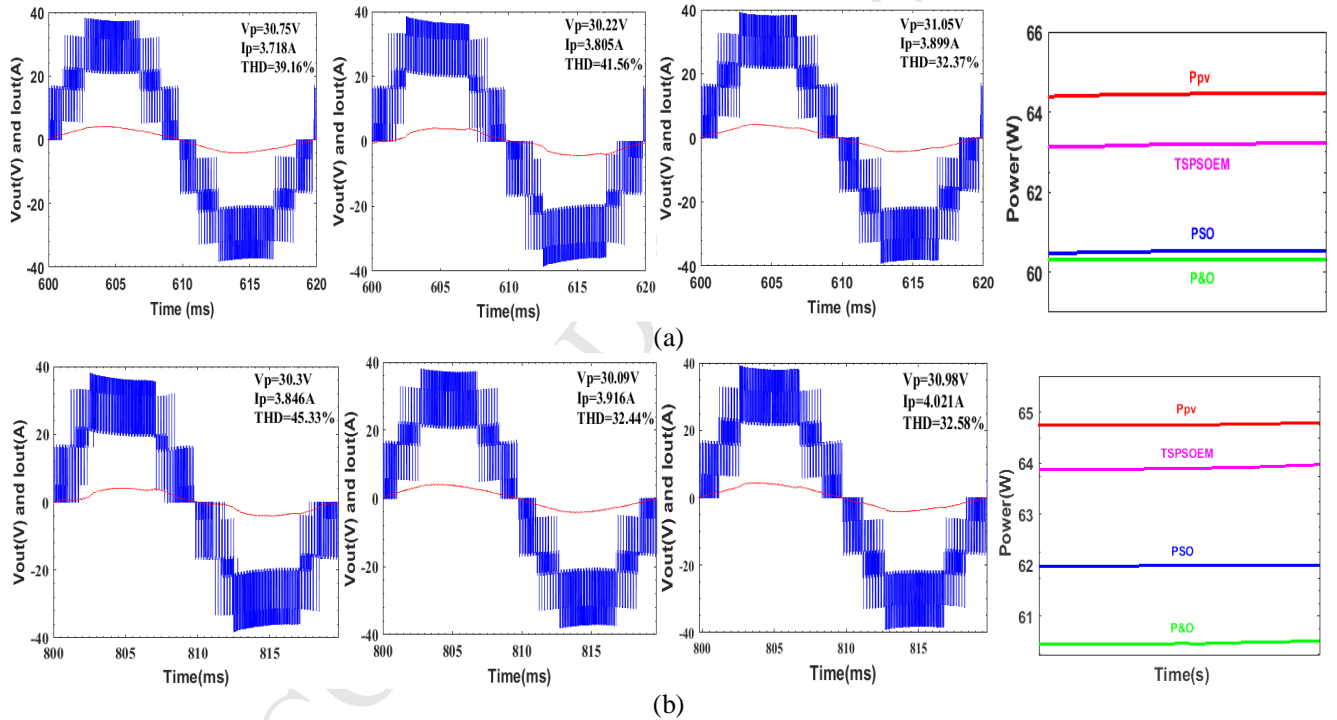

(a)

(b)

Figure 6 Output voltage and current waveforms of seven-level converter measured under the control by P&O method (column 1), the traditional PSO method (column 2) and the proposed algorithm (column 3), and output power curves of three methods (column 4), including sum of maximum power values found from the three sources (*Ppv*) (red line), the proposed method (pink line), the PSO method (blue line) and the P&O method (green line)
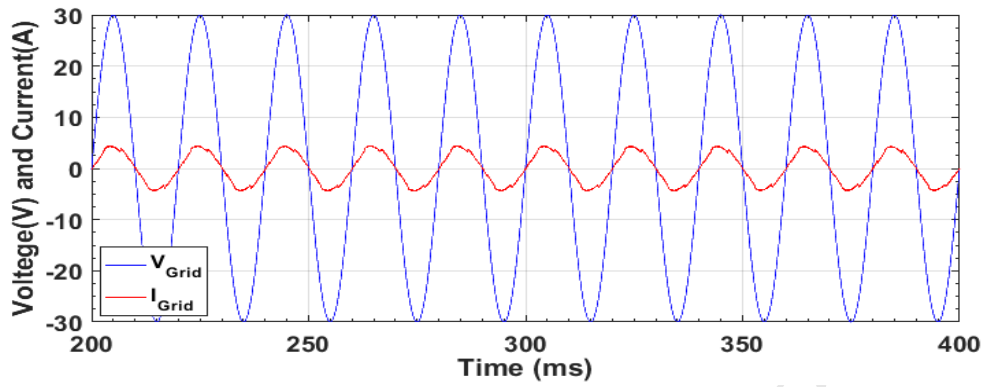
Figure 7 Current from PV system and grid voltage under unity power factor control by the proposed method in Case 2
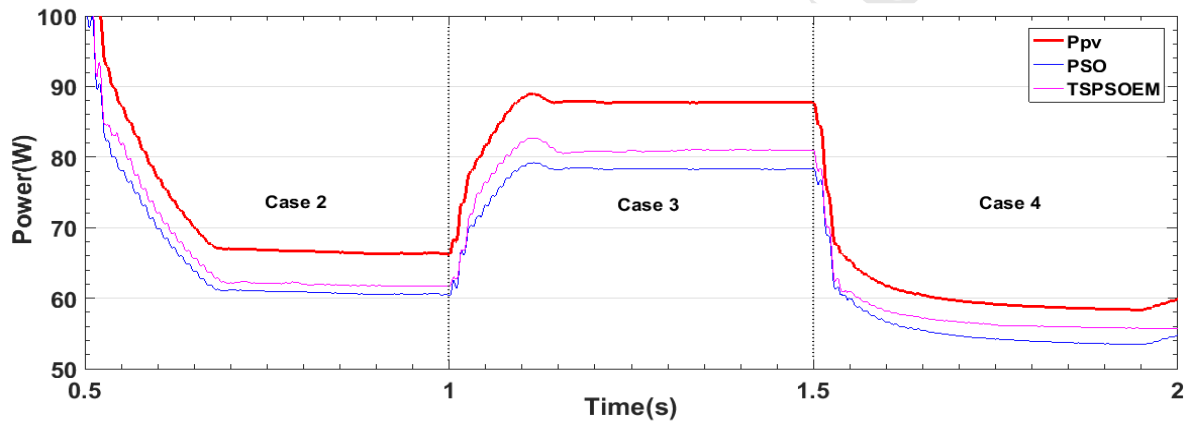

Figure 8 Output power curves of the two methods under fast transient variations of shading patterns

Highlights:

1. Grid-connected modular PV-converter system is presented.
2. A novel hybrid DMPPT algorithm for PV-converter PV system is proposed.
3. A PWM algorithm with permutation of PV sources is introduced.
4. The PV system is simulated for various conditions and results are analyzed.
5. The proposed algorithm is more accurate under fast changing weather conditions.